AFRL-RX-WP-JA-2015-0024

REFLECTION SPECTRA OF DISTORTED CHOLESTERIC LIQUID CRYSTAL STRUCTURES IN CELLS WITH INTERDIGITATED ELECTRODES (POSTPRINT)

Timothy J. White and Timothy J. Bunning
AFRL/RXAP

Mariacristina Rumi
Azimuth Corp

JULY 2014
Interim Report

AIR FORCE RESEARCH LABORATORY
MATERIALS AND MANUFACTURING DIRECTORATE
WRIGHT-PATTERSON AIR FORCE BASE, OH 45433-7750
AIR FORCE MATERIEL COMMAND
UNITED STATES AIR FORCE

NOTICE AND SIGNATURE PAGE

Using Government drawings, specifications, or other data included in this document for any purpose other than Government procurement does not in any way obligate the U.S. Government. The fact that the Government formulated or supplied the drawings, specifications, or other data does not license the holder or any other person or corporation; or convey any rights or permission to manufacture, use, or sell any patented invention that may relate to them.

This report was cleared for public release by the USAF 88th Air Base Wing (88 ABW) Public Affairs Office (PAO) and is available to the general public, including foreign nationals.

Copies may be obtained from the Defense Technical Information Center (DTIC) (http://www.dtic.mil).

AFRL-RX-WP-JA-2015-0024 HAS BEEN REVIEWED AND IS APPROVED FOR PUBLICATION IN ACCORDANCE WITH ASSIGNED DISTRIBUTION STATEMENT.

//Signature//

TIMOTHY J. WHITE
Photonic Materials Branch
Functional Materials Division

//Signature//

CHRISTOPHER D. BREWER, Chief
Photonic Materials Branch
Functional Materials Division

//Signature//

TIMOTHY J. BUNNING, Chief
Functional Materials Division
Materials and Manufacturing Directorate

This report is published in the interest of scientific and technical information exchange, and its publication does not constitute the Government's approval or disapproval of its ideas or findings.

REPORT DOCUMENTATION PAGE

Form Approved
OMB No. 074-0188

1. REPORT DATE (DD-MM-YYYY)	2. REPORT TYPE	3. DATES COVERED *(From – To)*
July 2014	Interim	24 December 2009 – 03 June 2014

4. TITLE AND SUBTITLE
REFLECTION SPECTRA OF DISTORTED CHOLESTERIC LIQUID CRYSTAL STRUCTURES IN CELLS WITH INTERDIGITATED ELECTRODES (POSTPRINT)

5a. CONTRACT NUMBER
FA8650-09-D-5434-0009

5b. GRANT NUMBER

5c. PROGRAM ELEMENT NUMBER
62102F

6. AUTHOR(S)
(see back)

5d. PROJECT NUMBER
3002

5e. TASK NUMBER

5f. WORK UNIT NUMBER
X092

7. PERFORMING ORGANIZATION NAME(S) AND ADDRESS(ES)
(see back)

8. PERFORMING ORGANIZATION REPORT NUMBER

9. SPONSORING / MONITORING AGENCY NAME(S) AND ADDRESS(ES)
Air Force Research Laboratory
Materials and Manufacturing Directorate
Wright Patterson Air Force Base, OH 45433-7750
Air Force Materiel Command
United States Air Force

10. SPONSOR/MONITOR'S ACRONYM(S)
AFRL/RXAP

11. SPONSOR/MONITOR'S REPORT NUMBER(S)
AFRL-RX-WP-JA-2015-0024

12. DISTRIBUTION / AVAILABILITY STATEMENT
Distribution A. Approved for public release; distribution unlimited. This report contains color.

13. SUPPLEMENTARY NOTES
PA Case Number: 88ABW-2014-2127, Clearance Date: 8 May 2014. Journal article published in Optics Express,. 2014 Jun 30;22(13):16510-9. © 2014 Optical Society of America. The U.S. Government is joint author of the work and has the right to use, modify, reproduce, release, perform, display or disclose the work. The final publication is available at doi. 10.1364/OE.22.016510.

14. ABSTRACT
We studied the appearance of second- and third-order Bragg reflections in cholesteric liquid crystals (CLCs) in cells where the electric field was perpendicular to the helical axis. Second-order reflections with reflectance values as large as 80% of the first-order one were observed in the gap regions of alignment cells with interdigitated electrodes for CLC mixtures with pitches in the range 0.5-1.0 μ m upon application of a field. The characterization was enabled by local probing of the CLC using a microspectrophotometer. LC cells that are transparent in the visible spectrum in the off-state and become colored upon application of a field due the second- or third-order reflection band appearance were demonstrated. The spectral position of the higher-order Bragg reflections can also be tuned by adjusting the magnitude of the electric field.

15. SUBJECT TERMS
liquid crystals, liquid-crystal devices, Bragg reflectors, optical properties, chiral media

16. SECURITY CLASSIFICATION OF:			17. LIMITATION OF ABSTRACT	18. NUMBER OF PAGES	19a. NAME OF RESPONSIBLE PERSON *(Monitor)*
					Timothy J. White
a. REPORT	b. ABSTRACT	c. THIS PAGE	SAR	14	19b. TELEPHONE NUBER *(include area code)*
Unclassified	Unclassified	Unclassified			(937) 255-9551

REPORT DOCUMENTATION PAGE Cont'd

6. AUTHOR(S)

Timothy J. White and Timothy J. Bunning - Materials and Manufacturing Directorate, Air Force Research Laboratory, Functional Materials Division

Mariacristina Rumi - Azimuth Corp.

7. PERFORMING ORGANIZATION NAME(S) AND ADDRESS(ES)

AFRL/RXAP
Air Force Research Laboratory
Materials and Manufacturing Directorate
Wright-Patterson Air Force Base, OH 45433-7750

Azimuth Corp.
4134 Linden Avenue
Dayton, Ohio 45432

Reflection spectra of distorted cholesteric liquid crystal structures in cells with interdigitated electrodes

Mariacristina Rumi,[1,2] Timothy J. White,[1] and Timothy J. Bunning[1,*]

[1]*Materials and Manufacturing Directorate, Air Force Research Laboratory, Wright Patterson Air Force Base, OH 45433, USA*

[2]*Azimuth Corporation, 4134 Linden Ave., Ste. 300, Dayton, OH 45432, USA*

[*]*timothy.bunning@us.af.mil*

Abstract: We studied the appearance of second- and third-order Bragg reflections in cholesteric liquid crystals (CLCs) in cells where the electric field was perpendicular to the helical axis. Second-order reflections with reflectance values as large as 80% of the first-order one were observed in the gap regions of alignment cells with interdigitated electrodes for CLC mixtures with pitches in the range 0.5-1.0 μm upon application of a field. The characterization was enabled by local probing of the CLC using a microspectrophotometer. LC cells that are transparent in the visible spectrum in the off-state and become colored upon application of a field due the second- or third-order reflection band appearance were demonstrated. The spectral position of the higher-order Bragg reflections can also be tuned by adjusting the magnitude of the electric field.

OCIS codes: (160.3710) Liquid crystals; (230.3720) Liquid-crystal devices; (230.1480) Bragg reflectors; (160.4760) Optical properties; (160.1585) Chiral media.

References and links

1. P. G. de Gennes, *The Physics of Liquid Crystals* (Clarendon Press, 1974).
2. P. G. de Gennes, "Calcul de la distorsion d'une structure cholesterique par un champ magnetique," Solid State Commun. **6**(3), 163–165 (1968).
3. V. A. Belyakov, V. E. Dmitrienko, and V. P. Orlov, "Optics of cholesteric liquid crystals," Sov. Phys. Usp. **22**(2), 64–88 (1979).
4. L. M. Blinov and V. G. Chigrinov, *Electrooptic effects in liquid crystal materials* (Springer, 1994), Chap. 6.
5. R. Dreher, "Reflection properties of distorted cholesteric liquid crystals," Solid State Commun. **12**(6), 519–522 (1973).
6. S. Shtrikman and M. Tur, "Optical properties of the distorted cholesteric structure," J. Opt. Soc. Am. **64**(9), 1178–1189 (1974).
7. S. C. Chou, L. Cheung, and R. B. Meyer, "Effects of a magnetic field on the optical transmission in cholesteric liquid crystals," Solid State Commun. **11**(8), 977–981 (1972).
8. S. C. Chou, L. Cheung, and R. B. Meyer, "Errata to "Effects of a magnetic field on the optical transmission in cholesteric liquid crystals"," Solid State Commun. **13**, iv (1973).
9. D. W. Berreman and T. J. Scheffer, "Bragg reflection of light from single-domain cholesteric liquid crystal films," Phys. Rev. Lett. **25**(9), 577–581 (1970).
10. R. Dreher and G. Meier, "Optical properties of cholesteric liquid crystals," Phys. Rev. A **8**(3), 1616–1623 (1973).
11. L. M. Blinov, S. V. Belyaev, and V. A. Kizel, "High-order reflections from a cholesteric helix induced by an electric field," Phys. Lett. **65**(1), 33–35 (1978).
12. D. J. Broer, G. N. Mol, J. A. M. M. van Haaren, and J. Lub, "Photo-induced diffusion in polymerizing chiral-nematic media," Adv. Mater. **11**(7), 573–578 (1999).
13. M. Rumi, V. P. Tondiglia, L. V. Natarajan, T. J. White, and T. J. Bunning, "Non-uniform helix unwinding of cholesteric liquid crystals in cells with interdigitated electrodes," ChemPhysChem **15**(7), 1311–1322 (2014).
14. M. Rumi, V. P. Tondiglia, L. V. Natarajan, T. J. White, and T. J. Bunning, "Effects of in-plane electric fields on the optical properties of cholesteric liquid crystals," Proc. SPIE **8828**, 882817 (2013).
15. R. Dreher, "Remarks on the distortion of a cholesteric structure by a magnetic field," Solid State Commun. **13**(10), 1571–1574 (1973).
16. S. V. Belyaev and L. M. Blinov, "Step unwinding of a spiral in a cholesteric liquid crystal," JETP Lett. **30**, 99–103 (1979).

Received 9 May 2014; accepted 3 Jun 2014; published 26 Jun 2014

17. J. V. Gandhi, X.-D. Mi, and D.-K. Yang, "Effect of surface alignment layers on the configurational transitions in cholesteric liquid crystals," Phys. Rev. E. **57**(6), 6761–6766 (1998).
18. H. G. Yoon, N. W. Roberts, and H. F. Gleeson, "An experimental investigation of discrete changes in pitch in a thin, planar, chiral nematic device," Liq. Cryst. **33**(4), 503–510 (2006).
19. M. Rumi, V. P. Tondiglia, L. V. Natarajan, T. J. White, and T. J. Bunning, "Local optical spectra and texture for chiral nematic liquid crystals in cells with interdigitated electrodes," Mol. Cryst. Liq. Cryst. (Phila. Pa.) (to be published), doi:10.1080/15421406.2014.917825.
20. H. Xianyu, S. Faris, and G. P. Crawford, "In-plane switching of cholesteric liquid crystals for visible and near-infrared applications," Appl. Opt. **43**(26), 5006–5015 (2004).
21. A. M. Scarfone, I. Lelidis, and G. Barbero, "Cholesteric-nematic transition induced by a magnetic field in the strong-anchoring model," Phys. Rev. E Stat. Nonlin. Soft Matter Phys. **84**(2), 021708 (2011).
22. J. Li, C.-H. Wen, S. Gauza, R. Lu, and S.-T. Wu, "Refractive indices of liquid crystals for display applications," J. Disp. Technol. **1**(1), 51–61 (2005).
23. G. Durand, L. Leger, F. Rondelez, and M. Veyssie, "Magnetically induced cholesteric-to-nematic phase transition in liquid crystals," Phys. Rev. Lett. **22**(6), 227–228 (1969).
24. T.-H. Lin, H.-C. Jau, C.-H. Chen, Y.-J. Chen, T.-H. Wei, C.-W. Chen, and A. Y.-G. Fuh, "Electrically controllable laser based on cholesteric liquid crystal with negative dielectric anisotropy," Appl. Phys. Lett. **88**(6), 061122 (2006).
25. R. A. M. Hikmet and H. Kemperman, "Electrically switchable mirrors and optical components made from liquid-crystal gels," Nature **392**(6675), 476–479 (1998).
26. N. Tamaoki and T. Kamei, "Reversible photo-regulation of the properties of liquid crystals doped with photochromic compounds," J. Photochem. Photobiol., C **11**(2-3), 47–61 (2010).
27. T. J. White, M. E. McConney, and T. J. Bunning, "Dynamic color in stimuli-responsive cholesteric liquid crystals," J. Mater. Chem. **20**(44), 9832–9847 (2010).
28. R. S. Pindak, C.-C. Huang, and J. T. Ho, "Divergence of cholesteric pitch near a smectic-A transition," Phys. Rev. Lett. **32**(2), 43–46 (1974).
29. R. B. Meyer, F. Lonberg, and C.-C. Chang, "Cholesteric liquid crystal smart reflectors," Mol. Cryst. Liq. Cryst. (Phila. Pa.) **288**, 47–61 (1996).

1. Introduction

A cholesteric liquid crystal (CLC) in a planar texture acts as a one-dimensional Bragg filter. For light incident along the normal to the cell (parallel to the helical axis), the center of the Bragg diffraction, $\lambda_{(1)}$, occurs at [1]:

$$\lambda_{(1)} = \tilde{n}\, p(0) \tag{1}$$

where $\tilde{n}$ is the average refractive index of the medium and $p(0)$ is the pitch of the helix in the absence of external fields. It is known that when an electric field is applied perpendicular to the helical axis of a CLC, materials with positive dielectric anisotropy and in a planar conformation experience an elongation of the pitch but retain the planar texture, leading to a redshift of the diffraction peak [1–3]. The pitch diverges to infinity for fields approaching the critical value E_c, which depends on the physical properties of the liquid crystal (pitch, elastic constant, dielectric anisotropy) [1, 4]. This pitch increase is accompanied by a deformation of the helical structure so that the angle formed by the liquid crystal director with a reference axis in the plane of the substrate is no longer proportional to the coordinate along the helical axis. Under these conditions, Bragg reflections of all orders are in principle active for light at normal incidence and their wavelengths are given by [3, 5, 6]:

$$m\lambda_{(m)}(E) = \tilde{n}\, p(E) \tag{2}$$

where m is an integer and $p(E)$ is the pitch for an electric field of magnitude E perpendicular to the helical axis. For $E = 0$ and $m = 1$, Eq. (2) reduces to Eq. (1). For the ideal helix ($E = 0$), selection rules restrict Bragg reflection to the first order only. A situation similar to that described by Eq. (2) is realized when a magnetic field is applied perpendicular to the helical axis [6–8]. Other types of deformation of the helical structure also affect the selection rules for diffraction from a CLC layer and can result in activation of modes with $m > 1$ [5]. In addition, Bragg reflections with $m > 1$ are active for unperturbed helices probed at inclined incidence (in this case $\lambda_{(m)}$ depends also on the incidence angle) [3, 9, 10]. Calculations of the light propagation through deformed helices have shown that the diffraction efficiency for high

Received 9 May 2014; accepted 3 Jun 2014; published 26 Jun 2014

order modes can be large and have a different polarization dependence with respect to the m = 1 mode [3, 7, 10].

Few experimental reports are available on field-induced high-order modes; when present, the measured efficiencies of these modes were small. In the early work by Blinov *et al.* [11], the second order mode was observed for CLCs with a pitch between 1 and 2.5 μm although a high-sensitivity setup was needed to allow the detection of the weak signals. In that report, the change in transmittance associated with the second order mode was found to scale as $E^{3.5}$ and to have a magnitude of ~4% at 0.5 E_c. The same report mentioned that third- and fourth-order reflections were not observed in long pitch CLCs even though those modes would have been in the wavelength range of the detection system; this was ascribed to the low intensity expected for $m > 2$ modes. At least one report contains an appreciable second-order mode and a smaller, but measurable, third-order mode [12]. For this case, the deformation was the result of photo-induced diffusion during polymerization and as such was present without application of an electric or magnetic field.

Here we observe higher-order ($m > 1$) reflections for various CLC mixtures with the main (m = 1) reflection in the near-infrared range in cells with interdigitated electrodes (IDEs). These findings were made possible by measuring reflection spectra with spatial selectivity within the gap regions of the cell by use of a microspectrophotometer. We show that large reflectances for the second-order mode can be achieved in various samples in the center of the gap regions between electrodes. The efficiency of second-order reflections increases with the magnitude of the applied field and can become comparable to that of the first order reflection at high fields. Third-order reflection bands could also be observed in samples for which $\lambda_{(1)}/3$ is in the visible range. The reflectance of the second and third-order modes in these samples is large enough to yield changes in the visual color of the CLC in gap areas. This phenomenon may be used to fabricate filters that are transparent in a given wavelength range in the off-state (no electric field) but exhibit an electrically-induced and tunable reflection band when an electric field is applied.

2. Materials and experimental details

The compositions of the CLC mixtures used in this investigation are reported in Table 1. All compounds were obtained from Merck and used as received. The nematic liquid crystal hosts have positive dielectric anisotropy ($\Delta\varepsilon > 0$) in the frequency range of interest here. The IDE cells consist of two sets of linear and parallel electrodes patterned in the ITO layer on one of the glass substrates and where the other substrate is uniform glass. The cell parameters were: w = 56 μm, d = 44 μm, h = 4.8-5.0 μm, where w is the width of each electrode pad, d is the distance between electrodes (gap), and h is the cell thickness. The top and bottom substrates of the cell had been coated with polyimide and the rubbing direction was parallel to the electrodes. The cells were filled by capillary action while heated on a hot plate set slightly above the clearing temperature of the mixtures. For IDE cells, the electric field at the center of the gaps can be expressed as $E_{gap} = f\,V/d$, where V is the potential difference applied between the two sets of electrodes and f is a form factor that depends on the electrode dimensions and shape. For the cells used in this study, we estimated that f = 0.6, based on simulations of the electric field in an empty cell [13]. The gap electric field in V/μm is thus $E_{gap} \approx 0.0107\,V$ (with V in volts). The electric field was applied as a square wave at 1 kHz using a function generator (Agilent, model 33120A) and an amplifier (MTS, model M94100). The potential differences and electric fields quoted in the text are root-mean-square (rms) values.

Table 1. Composition of the Cholesteric Liquid Crystal Samples

Sample ID	*Nematic host*		*Chiral dopant*		$\lambda_{(1)}$	E_c
	type	*content* (wt%)	*type*	*content* (wt%)	(nm)	(V/μm)
#1	BL037	96	R1011	4	1217	2.82
#2	BL038	76	CB15	24	944	3.01
#3	E7	80	R811	20	835	4.15

Received 9 May 2014; accepted 3 Jun 2014; published 26 Jun 2014

Reflection spectra were obtained on a microspectrophotometer (CRAIC Technologies, model MSP 121) using a 36X objective and a sampling spot size of ca. 4 μm × 4 μm, averaging 2-10 acquisitions per spectrum and with a 2 s collection time per scan. Even at this collection time (the upper limit for the instrument), the counts at the edge of the detector range are small, resulting often in curved or noisy baselines at the short and long wavelength edges. The number of scans was kept relatively low in order to reduce the contribution of dark defects, which sometime formed during the measurement or moved across the probed area. Natural light was used in all cases. The spectra are reported relative to the reflectance of a flat aluminum mirror, which was used as a reference under the same illumination and collection conditions as the samples. However, because of some uncertainty in adjusting sample height at the focal plane of the objective for the reference and the sample specimens, we observed variations in reflectance values by a few percent in independent measurements on the same nominal sample. Measurements were conducted on a given sample sequentially at increasingly larger voltages, without turning the field off or changing the stage height between scans. As such, spectra obtained in the same measurement session are affected by smaller instrumental repeatability and changes in reflectance should represent actual variations in materials properties. It should be mentioned that, due to the use of a microscope objective to illuminate the sample, the incoming beam includes components forming a non-zero angle with the helical axis. In principle, the second-order mode could be present even in the unbiased sample. As we see no evidence of this mode at 0 V in the measured reflectance spectra for any of the samples, we infer that its efficiency over the cone angle of the excitation beam is below our detection limit.

Images were collected through a CCD camera attached to the same microscope and were recorded immediately before or after the measurement of a reflection spectrum at the center of the visual field. For the cell parameters used here, no significant difference was observed in reflection spectra obtained with illumination on the patterned or unpatterned substrates, as we discussed previously in [13]. The critical fields included in Table 1 are estimated from the lowest voltages for which no reflection was detected from the samples; their uncertainty is about ± 5%.

3. Results and discussion

3.1 Dependence of second-order mode reflectance on voltage

The magnitude and direction of the electric field is nonuniform in cells with IDEs. Thus, the response of the CLC when a potential difference is applied between the two sets of electrodes varies with location in the cell. We are interested in the behavior when the electric field is in the plane of the cell substrate, and thus perpendicular to the helix, which occurs only in the central region of the gaps between electrodes. A microspectrophotometer can be used to selectively probe the sample in various locations by choosing spot sizes small with respect to the electrode pattern dimensions. We have used this measurement tool to understand the effect of IDE cell geometry on the changes in reflection spectra of CLCs as a function of electric field strength [13]. The same microspectrophotometer was used in the current study and all the spectra reported here were obtained at the center of gap regions, within an area approximately 4 × 4 μm^2. The concentration of chiral dopant in each of the samples was chosen to yield a Bragg reflection in the absence of fields at wavelengths above 800 nm, so that the second-order band would be above the short-wavelength cutoff for our detector and glass substrates.

Received 9 May 2014; accepted 3 Jun 2014; published 26 Jun 2014

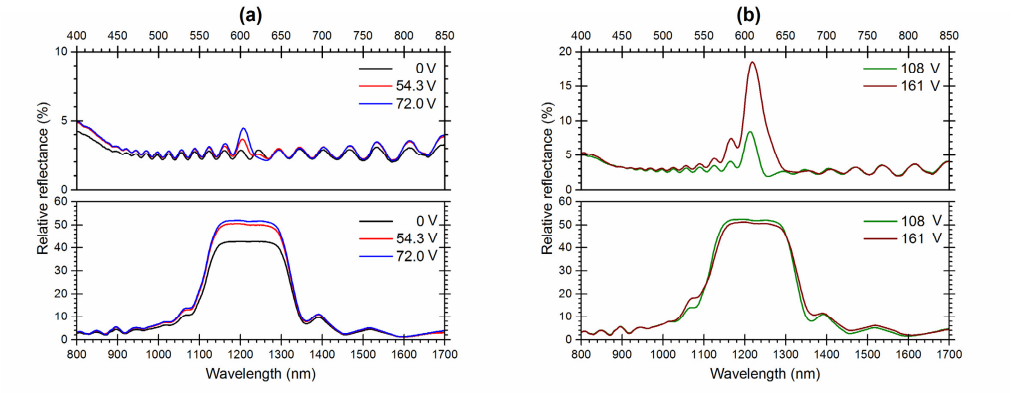

Fig. 1. Reflection spectra of sample **#1** in the range of the main reflection band (bottom graphs) and of the second-order reflection (top graphs) as a function of applied voltage: (a) 0 V, 54 V (0.21 E_c), 72 V (0.27 E_c); (b) 108 V (0.41 E_c), 161 V (0.61 E_c).

The first-order reflection band for sample **#1** is centered at 1217 nm and no other features are present in the spectrum at zero voltage apart from a small modulation of the baseline signal due to reflections at the cell substrates/CLC interfaces [black trace in Fig. 1(a)]. When a voltage is applied, starting at about 50 V, a weak reflection band appears around half the wavelength of the main band [606 nm in the case of Fig. 1(a)] and it increases in intensity with increasing potential difference [Fig. 1(b)]. This band is due to the activation of the second-order Bragg reflection once the cholesteric helix becomes deformed in the presence of the electric field. A similar behavior was observed for samples **#2** and **#3**. For the voltage range included in Fig. 1, there were no changes in the shape and position of the first-order reflection band. The wavelength dependence with voltage of the $m = 1$ and 2 modes will be discussed in Section 3.2.

The magnitude of the second-order band continues to increase as a function of electric field up to 0.7-0.8 E_c for all three samples (results for **#1** and **#2** are given in Fig. 2; the experimental estimate of E_c for each of the samples is given in Table 1). The reflectance values follow approximately a power law $a(E/E_c)^b$ with $2 < b < 3$ for $E < 0.7\ E_c$. We find that the values of the exponent b differ from sample to sample ($b = 2.9$, 2.3, and 2.6 for sample **#1**, **#2**, and **#3**, respectively) and that they are smaller but on the same order as the value reported by Blinov *et al.* ($b = 3.5$) [11]. The reason for the spread in b values is unclear, but it could be related to an actual dependence of the mode efficiency on material parameters or to the formation of defects and multidomain structures (these were observed more prominently in sample **#3** than in samples **#1**-**2**). Calculations of light propagation in deformed structures over a wide range of field and materials parameters should help in identifying the origin of the variation. Calculation results currently available in the literature were obtained on a small set of field magnitudes and materials [5–7]. If present, defects often appear in microscope images as dark lines (weak or no reflectance) spanning the gap approximately along the field direction and they are not static. If these move across the measurement spot during the course of a spectrum collection, the effective reflectance would appear lower than that of the domains on either side of the defects.

Received 9 May 2014; accepted 3 Jun 2014; published 26 Jun 2014

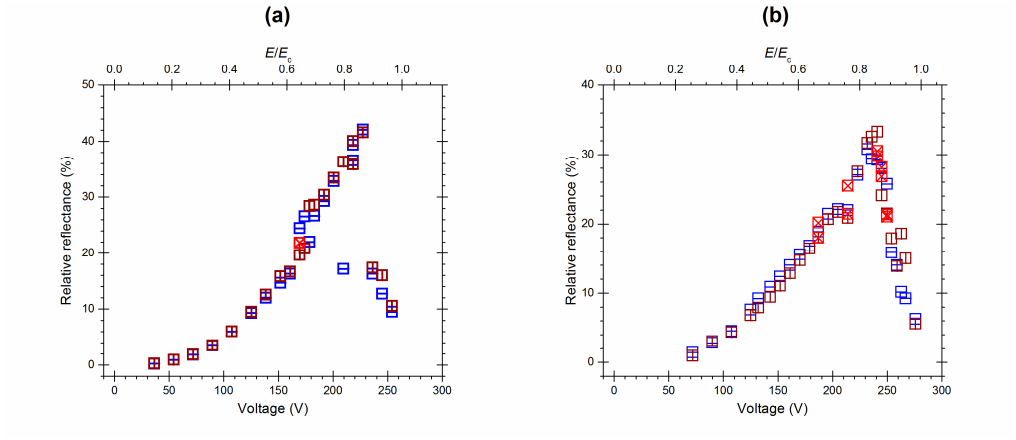

Fig. 2. Reflectance of the m = 2 band as a function of applied voltage: (a) sample **#1**, (b) sample **#2**. For any given voltage, the electric field relative to E_c can be read in the scale at the top of the graph. The reflectance values (relative to aluminum) are reported after subtraction of the signal for the 0 V case at the same wavelength. Differently colored symbols correspond to measurements at three sample locations.

For fields above 0.8 E_c, the second-order band exhibited a drastic decrease in reflectance. This was often accompanied by a broadening of the bands and the appearance of a substructure consisting of a series of peaks and valleys, possibly due to interference. In this field range, the main reflection band at $\lambda_{(1)}(E)$ also became weaker and developed a structured bandshape. A larger number of faster moving defects were often observed in this field range.

All three samples exhibit large reflectance of the second-order mode (above 20%) over a range of voltages. The maximum reflectance was about 40% for sample **#1** [see Fig. 2(a)], 30% for sample **#2** [Fig. 2(b)], and 22% for sample **#3**. At 0.5 E_c, the reflectance of the m = 2 mode was on the order of 10% for samples **#1** and **2**. This is significantly larger than that for the case in [11]. We cannot exclude that the difference with the present case is ascribable to a material dependence of the efficiency. However, as we observed large reflectances in samples with different dopants and host components (see Table 1), the effect should not be particularly rare. We observed less efficient (10-15%) second-order reflection bands in IDE cells with smaller electrodes and gaps [14]. We believe the lower efficiency measured in our previous work is due to the fact that the electric field was not constant through the thickness of those cells. Field inhomogeneity, however, cannot account for low reflectances observed by Blinov *et al.* [11], as no IDEs were present in that case. 20 μm thick metal strips (200 to 500 μm apart) were used as both electrodes and spacers [11], suggesting that the field should have been constant throughout the cell.

3.2 Wavelength of second-order reflection band

As mentioned in the introduction, when an electric field is applied perpendicular to the axis of the CLC helix, the pitch is expected to extend and become infinite at E_c. A redshift of the first-order band is indeed observed in all samples (see Fig. 3 for data on samples **#1**-**2**). As can be seen from the graphs, the change in the reflection band position, and thus pitch, takes place in discrete steps, not continuously as a function of increasing voltage. This can occur in the case of strong anchoring at the two substrates of the cell, for which only an integer number of half pitches (the period of the band gap structure) can be accommodated in the thickness of the cell at any given voltage [15, 16]. The finite step in band position then corresponds to a decrease in the number of periods by one. In the absence of field, discrete changes in pitch due to boundary conditions have also been observed as a function of temperature and composition (see, for example, [17, 18]). We have recently reported on the experimental observation of the step-wise change in pitch as a function of electric field for a

Received 9 May 2014; accepted 3 Jun 2014; published 26 Jun 2014

sample equivalent to **#1** [19]. The current findings on samples **#2**-**3** indicate that this behavior can be easily observed in various CLC mixtures when the spectra are collected with spatial resolution within the gap between electrodes. In Fig. 3, the black dashed line represents the behavior expected for a system with weak anchoring, according to the derivation by de Gennes [2]. In the presence of strong anchoring the traces would instead be a series of step functions up to the critical field [15, 20, 21]. In Fig. 3, for simplicity, we draw only the curve describing the theoretical pitch variation for weak anchoring, setting the vertical asymptote at the first voltage value at which no reflection band was observed.

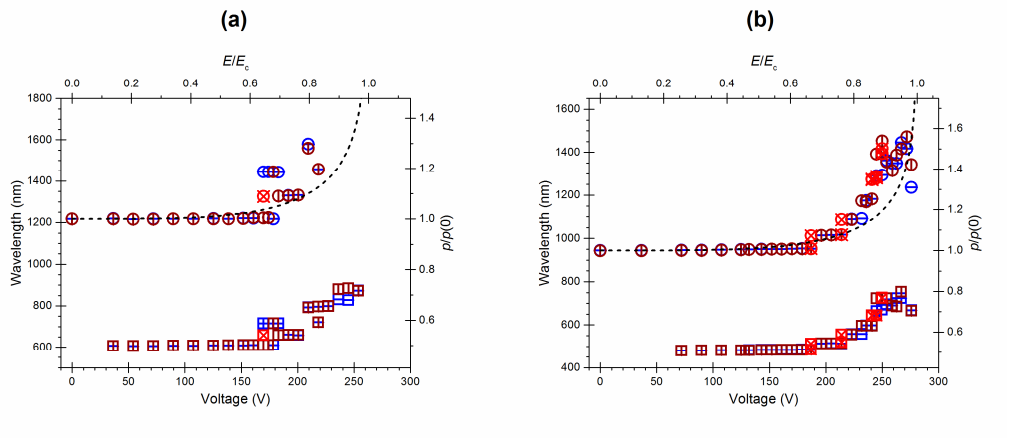

Fig. 3. Wavelength of the center of the first-order (circles) and second-order (squares) reflection bands: (a) sample **#1**, (b) sample **#2**. Differently colored symbols correspond to measurements at three sample locations, which were the same as for the data in Fig. 2. The black dashed line is for the de Gennes model.

The second-order mode appears at low voltages around $\lambda_{(1)}(0)/2$ and then shifts to longer wavelength in step with the first-order one as the voltage is increased (Fig. 3), in agreement with Eq. (2). It should be noted that in the case of sample **#1**, the first-order band moved outside the detector range for $V > 210$ V and thus Fig. 3(a) only reports data points for the second-order band at high voltages.

Close inspection of the position of the second-order bands shows that $\lambda_{(2)}(E)$ is not located exactly at $\lambda_{(1)}(E)/2$ but at slightly longer wavelengths. For example, the ratios $\lambda_{(2)}(E)/\lambda_{(1)}(E)$ were found to be 0.508 and 0.513 for samples **#2** and **#3**, respectively. Given the resolution of the spectrometer these ratios should be reliable to about ± 0.001 and thus the values for the two samples should be distinct. The deviation of the ratios from ½ is due to the dispersion of the refractive index. In fact, assuming a normal dispersion of the refractive index for $\lambda > \lambda_{(m)}(E)$, from Eq. (2) we can write for any given value of E:

$$\frac{\lambda_{(m)}(E)}{\lambda_{(1)}(E)} = \frac{\tilde{n}_{\lambda_{(m)}}}{m\,\tilde{n}_{\lambda_{(1)}}} > \frac{1}{m} \qquad (3)$$

where the subscript in $\tilde{n}$ indicates explicitly the wavelength at which it has to be evaluated. Using the parameters for a three-coefficient Cauchy model of the refractive index of E7 reported by Li *et al.* in [22], we estimate from Eq. (3) $\lambda_{(2)}(E)/\lambda_{(1)}(E) = 0.521$ for sample **#3** (a ratio of 0.513 would be expected for a sample with $\lambda_{(1)}(0) = 1.0$ μm). This number is larger than the experimental results. Small changes in the refractive index of the medium due to the presence of R811 in the mixture or some asymmetry in the shape of the reflection band, either because of the presence of multiple domains or a field-induced variation in polarization dependence of the reflectance, could account for the discrepancy.

Received 9 May 2014; accepted 3 Jun 2014; published 26 Jun 2014

3.3 Observation of m = 3 reflections

For the three samples investigated we could also observe a weak band around $\lambda_{(1)}(E)/3$ for at least part of the voltage range and we assign this to the third-order Bragg reflection. For sample **#1** [Fig. 4(a)] there is no third-order band at 0 V, as expected, but a new feature starts appearing around 200 V and moves to longer wavelengths when the position of the main reflection band is redshifted by increasing the applied voltage. At 227 V, the band magnitude is about 7% with respect to the baseline set by the 0 V trace. For the other two samples, $\lambda_{(1)}(0)/3$ is below the short-wavelength limit of the measurement system, so we could not investigate its behavior at low voltages. The band becomes detectable at voltages for which $\lambda_{(1)}(E)$ is above 1100 nm, as shown in Fig. 4(b) for sample **#2** at 236 and 250 V (in these spectra, the increases in reflectance above 500 nm correspond to the rising edge of the second-order band).

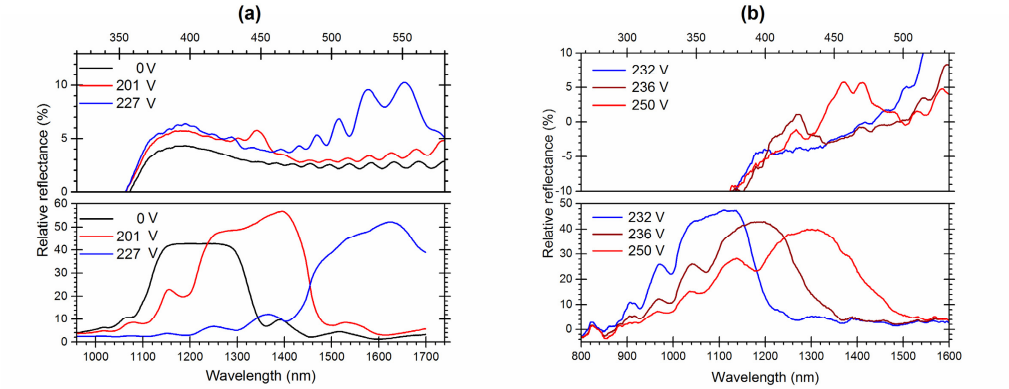

Fig. 4. Reflection spectra in the range of the main reflection band (bottom graphs) and the third-order mode (top graphs) at various voltages: (a) sample **#1** (227 V corresponds to 0.86 E_c); (b) sample **#2** (250 V corresponds to 0.89 E_c). The baseline for $\lambda < 450$ nm is not flat because of the low detector and lamp efficiency in this range and possibly a slightly different contribution from scattering for the sample and reference scans.

3.4 Tunable reflective devices with dark off-state

Because the second-order mode is not active at 0 V and the samples considered here have the main Bragg reflection in the near-infrared range, the cells appear dark to the eye in reflection in the as-prepared state. When a potential difference is applied between the electrode sets, the second-order mode becomes active, as discussed above, and the gap region assumes the color corresponding to wavelength $\lambda_{(2)}(E)$, which is in the visible range. The reflectance of the second-order mode is large enough for the coloring to be seen by eye through the eyepiece and be easily recorded by a CCD camera mounted on the microscope, as shown in the images in Fig. 5(c-d) for two of the samples. As the helix unwinds with increasing voltage, $\lambda_{(2)}(E)$ shifts toward longer wavelengths, as discussed in the previous section [see spectra in Fig. 5(a)-5(b)].

For all samples and most voltage values, the section of the gap regions bordering with the electrodes appear to have a different color from that of the central region of the gap. For example, for sample **#2**, in the second image from the left in Fig. 5(d) (170 V), the gap center is blue with green stripes on either side. This is due to the fact that the electric field strength increases going from the center to the edges of the gap regions, and thus the cholesteric helix is unwound to a larger extent in the edge regions [16]. The leftmost and rightmost regions in each of the images are parts of the electrodes and remain relatively dark, with some texture visible at finite voltages due to the focal conic state of the CLC. It should be mentioned that the gap in the rightmost image in Fig. 5(c) (227 V) appears green because of the presence of the third-order band around 520 nm, which can be seen in the corresponding spectrum [see

Received 9 May 2014; accepted 3 Jun 2014; published 26 Jun 2014

also Fig. 4(a)], as the second-order band is already in the NIR range (about 800 nm) at this voltage. The third-order mode, even if rather weak, contributes to the gap color also at 219 V. This is the reason for the apparent deviation from a red-shift in color in the images collected for sample **#1** [Fig. 5(c)].

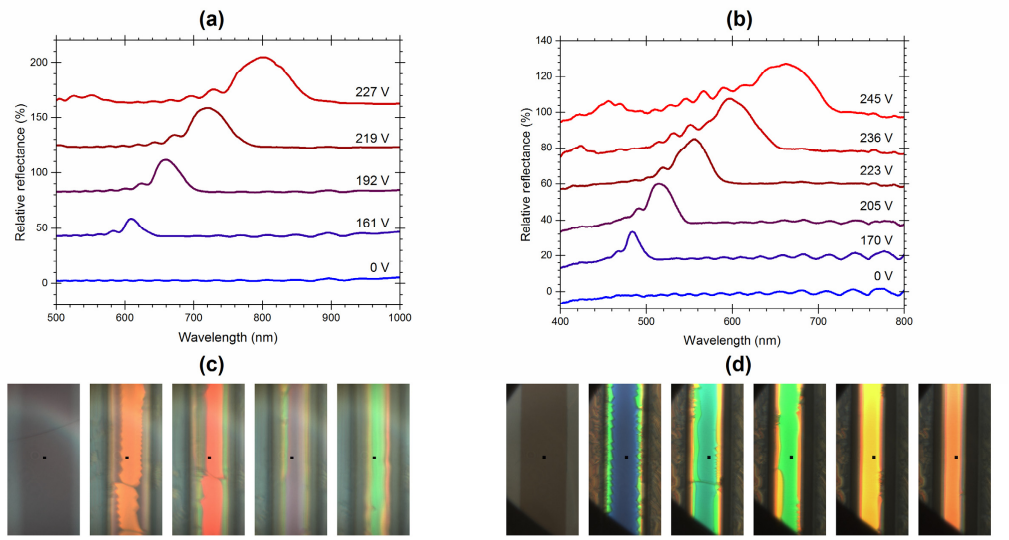

Fig. 5. (Top) Reflection spectra at gap center at selected voltages for (a) sample **#1** (227 V corresponds to 0.86 E_c) and (b) sample **#2** (245 V corresponds to 0.87 E_c). The spectra are displaced vertically for clarity. (Bottom) Microscope images (natural light, reflection mode) of sections of the same gap region as the spectra (spectra were collected in the dark squares in the center of the images) and of the adjacent electrodes for the same voltage values as the spectra shown (with voltage increasing from left to right for each of the two samples): (c) sample **#1**, (d) sample **#2**. The size of each image is 90 μm × 185 μm.

The data in Fig. 5 show that diffraction in the $m = 2$ order can constitute the basis for a reflective electro-optic device that can be turned on and then tuned by an electric field. The device would be transparent in the off-state (dark in reflection mode). This is the main difference with respect to a CLC device that is based on the main ($m = 1$) Bragg reflection: the latter would still display a reflection band tunable toward longer wavelengths as a function of increasing voltage, but the band would also be present in the off-state. For applications in the visible portion of the spectrum, this alternative device would thus be colored in the off-state. In principle, a short-pitch CLC mixture could be used, so that $\lambda_{(1)}(0)$ is in the UV range and the reflection band enters the visible range at some higher voltage. In this situation, however, because of the short pitch and the inverse dependence of E_c on pitch [1, 23], the voltage needed to obtain a certain tuning range would be approximately twice that required by the scheme based on second-order modes. Any other device based on CLCs with a planar configuration cannot result in a true switch-on of a reflection band in response to an external stimulus, but it may be possible to design a system for which the band is moved from outside the region of interest. For example, a blue-shift of the reflection band can be obtained in CLCs with $\Delta\varepsilon > 0$ and top/bottom electrode cells, with or without polymer stabilization [24, 25], but the tuning ranges are typically small and significant scattering is also present. Light [26, 27] and temperature [28, 29] could also be used to move the reflection band in and out of the region of interest, but the response times are typically longer.

As discussed in Section 3.2, for all three samples we observed discrete changes in pitch and thus in the reflection band position for all orders. This would limit the applicability of the devices to situations where continuous tunability is not required. The discreteness of the changes, though, could provide more stability against voltage fluctuations or non-uniformity of electrode pattern with respect to a continuous pitch variation with field. For sample **#2**, five

Received 9 May 2014; accepted 3 Jun 2014; published 26 Jun 2014

distinct colors could be obtained in the visible range [Fig. 5(d)]. The device described here could be in principle used as a tunable reflective filter. Due to the presence of electrodes, the usable area of the device is smaller than the total area of the system, reducing the overall efficiency of the device at any voltage, and the regions above the electrode provide scattering background signal, which could decrease the contrast between the in-band and out-of-band reflectances. Both issues could be addressed, at least in part, if the device is used in combination with a lens array with the same periodicity as the electrode pattern, to enhance the fraction of incoming light reaching the gap regions.

4. Conclusions

Measurements of reflection spectra selectively from the gap regions of cells with interdigitated electrodes allowed us to determine that, in many CLC mixtures, electric field induced second- and third-order Bragg modes can exhibit large reflectances. In selected voltage ranges, reflectances of 30-40% for natural light have been recorded using a microspectrophotometer to spatially measure local reflectivity. This suggests that the stop band capabilities of periodic helicoidal structures deformed by electric fields can be rather efficient. In addition to providing information on the intrinsic properties of this type of periodic structure as a function of electric field, this study suggests that higher-order modes may be strong enough to be exploited in electro-optic devices operating in a different manner from those based on the first-order mode.

Acknowledgments

This work was funded by the Air Force Office of Scientific Research and the Materials and Manufacturing Directorate of the Air Force Research Laboratory. We thank Prof. Deng-Ke Yang, Kent State University, for kindly providing the IDE cells.

Received 9 May 2014; accepted 3 Jun 2014; published 26 Jun 2014